

## Fast versus conventional HAADF-STEM tomography: advantages and challenges

Electron tomography has evolved into a powerful technique to study the three-dimensional (3D) structure of functional nanomaterials. Conventionally, electron tomography experiments are based on acquiring tilt series of projection images with an increment of 1-2° over an angular range that is as large as possible. Although the acquisition of such a tilt series is mostly automated, even under ideal conditions approximately 1 hour is required to obtain all 2D projection images. This is clearly a major drawback when a large number of samples needs to be investigated or when dynamic effects appear during in-situ experiments. It is furthermore clear that 3D studies of radiation sensitive materials are extremely challenging since samples will degrade when long acquisition times are required. One of the emerging challenges in the field of electron tomography is therefore to accelerate the acquisition of tilt series for tomography. At the same time, the quality of the tomographic reconstructions should be maintained and enable one to obtain reliable and quantitative parameters such as e.g. particle size and surface morphology.

Recently, first attempts were made to accelerate the acquisition process of electron tomography tilt series [1,2] in TEM mode. Since we here investigate crystalline gold (Au) nanoparticles, HAADF-STEM rather than TEM should be used to fulfill the projection requirement for tomography [3]. Therefore we expanded upon this research and introduced fast HAADF-STEM tomography [4]. By continuously tilting the holder and simultaneously acquiring projection images while focusing and tracking the particle, the total acquisition time for a HAADF-STEM tilt series can be reduced by a factor of 10. We will present the fast acquisition strategy and all post processing steps involved to reduce artefacts and to obtain a reconstruction from the ‘fast’ dataset.

To validate the fast acquisition approach and the involved data processing, conventional and fast tomographic series were acquired for a series of Au nanoparticles with different shapes. 3D reconstructions were calculated for each series and compared in a qualitative and quantitative manner. In **Figure 1.a-b** and **1d-e** reconstructions obtained from a conventional and fast acquisition are visualized for a Au nanodecahedron and a Au nanostar. **Figure 1.c** and **1.f**, display orthoslices through the absolute difference between both reconstructions, after segmentation. This highlights voxels that were misclassified in the segmented reconstruction of the ‘fast’ data in comparison to the segmented reconstruction obtained from the conventional data. Based on a qualitative comparison and a visualization of the misclassified pixels (**Figure 1.c** and **1.f**), we conclude good agreement between the overall morphology of the nanoparticles as obtained using conventional and fast HAADF-STEM tomography. It should hereby be noted that the acquisition time for the fast series was reduced to approximately 4 minutes. This means that fast HAADF-STEM tomography has great potential for the further combination with in-situ studies [4–6].

The quantitative comparison is based on the shape error, which was calculated as a weighted sum over absolute differences between the segmented reconstructions:

$$E_s = \frac{\sum |Rec_{fast}^{seg} - Rec_{conv}^{seg}|}{\sum Rec_{conv}^{seg}} * 100 \quad [1]$$

$Rec_{fast}^{seg}$  and  $Rec_{conv}^{seg}$  refer to the segmented 3D reconstructions of the fast- and conventional series respectively. The sum over  $Rec_{conv}^{seg}$  defines the volume of the conventional reconstruction. In this way the shape error expresses the relative amount of misclassified voxels in the segmented reconstruction of the ‘fast’ dataset in comparison to the segmented

reconstruction obtained from the conventionally acquired data. For the Au nanodecahedron a shape error of only  $3.42 \pm 0.01 \%$  was found. The conventional reconstruction hereby served as the ground truth. For the anisotropic Au nanostar, the shape error increased to  $6.99 \pm 0.01 \%$ . This shows that overall the error between both remains limited, especially when the nanoparticles have a simple 3D geometry. The remaining differences are related to the fact that the object of interest is continuously tilting during the acquisition of a single projection image. In this contribution, we will discuss several strategies to overcome this limitation.

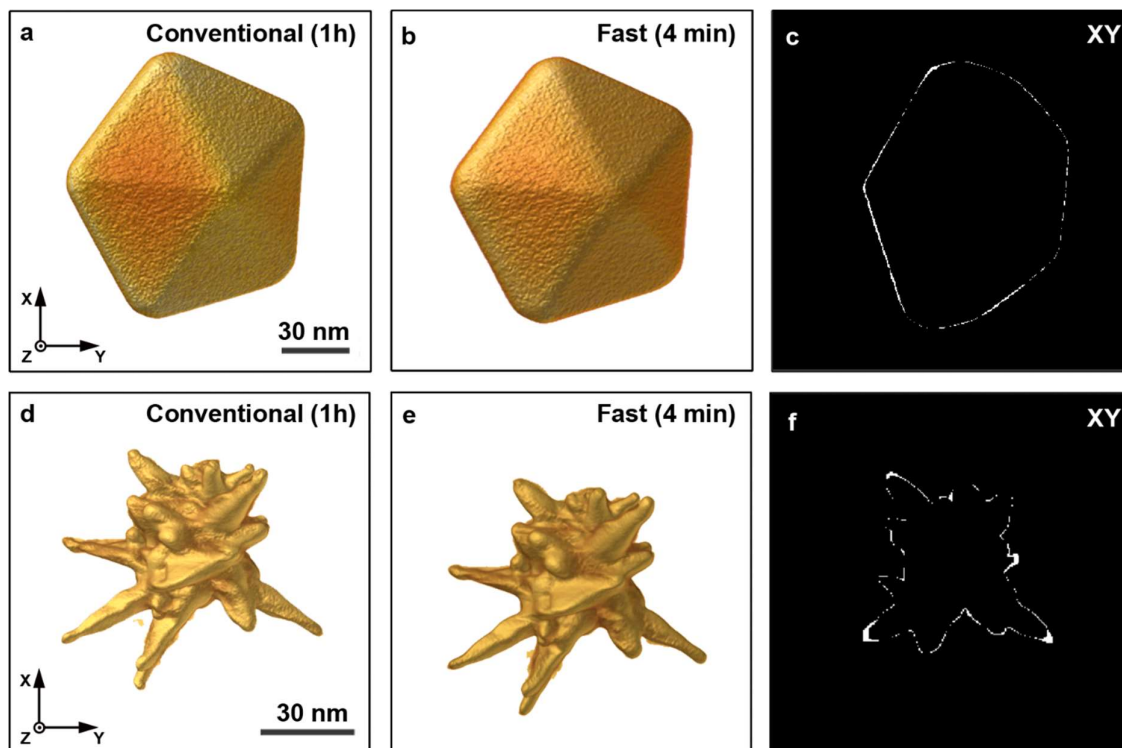


**Figure 1:** (a-b) 3D rendering of the reconstruction from respectively the conventionally and fast acquired projection images of a Au platelet with pentagonal symmetry. (c) XY orthoslice through the absolute difference between both reconstructions after segmentation. (d-e) 3D rendering of the reconstruction from respectively the conventionally and fast acquired projection images of a Au anisotropic nanostar. (f) XY orthoslice through the absolute difference between both reconstructions after segmentation.

## Conclusion

We implemented a methodology to perform fast electron tomography in HAADF-STEM mode, which allowed us to greatly reduce the total acquisition time of a tomographic acquisition. We show that by using dedicated processing there is near to no difference in reconstruction quality for isotropic nanoparticles. For anisotropic nanoparticles with a more complex shape, the discrepancy increases. Strategies to reduce this deviation will be presented.

## References

- [1] V. Migunov, H. Ryll, X. Zhuge, M. Simson, L. Strüder, K. J. Batenburg, L. Houben, R. E. Dunin-Borkowski, *Sci. Rep.* **2015**, 5, 14516.
- [2] L. Roiban, S. Li, M. Aouine, A. Tuel, D. Farrusseng, T. Epicier, *J. Microsc.* **2018**, 269, 117.
- [3] P. A. Midgley, M. Weyland, *Ultramicroscopy* **2003**, 96, 413.

[4] H. Vanrompay, E. Bladt, W. Albrecht, A. Béché, M. Zakhozheva, A. Sánchez-Iglesias, L. M. Liz-Marzán, S. Bals, *Nanoscale* **2018**, *10*, 22792.

[5] W. Albrecht, E. Bladt, H. Vanrompay, J. D. Smith, S. E. Skrabalak, S. Bals, *ACS Nano* **2019**, *13*, 6522.

[6] A. Skorikov, W. Albrecht, E. Bladt, X. Xie, J. E. S. Van Der Hoeven, A. Van Blaaderen, S. Van Aert, S. Bals, *ACS Nano* **2019**, DOI 10.1021/acsnano.9b06848.